

A Fully Automated Method for Spinal Canal Detection in Computed Tomography Images

Antonio Díaz-Parra, Estanislao Arana, and David Moratal, *Senior Member, IEEE*

Abstract— This work presents a new automated method for spinal canal detection in Computed Tomography (CT) images. It uses both 2D and 3D information and the algorithm extracts the spinal canal automatically. The procedure can be divided into three main steps. Firstly, a thresholding and a set of morphological operations were applied. Secondly, 3D connectivity analysis was defined to extract the objects forming part of the spinal canal. Finally, the centroid of each slice constituting the *spinal canal* object was computed. Furthermore, interpolation and extrapolation of data were performed, if required. The method was applied on two different groups, each one coming from different acquisition systems. A total of 25 patients and 8704 images were used. An experienced radiologist evaluated the method qualitatively supporting the utility of it, as all extracted points fell into the spinal canal. Therefore, our method was able to reduce the workload and detect spinal canal objectively. We expect to carry out a quantitative evaluation in our future research. The qualitative outcome of this work suggests promising results.

I. INTRODUCTION

Computed Tomography (CT) and Magnetic Resonance Imaging (MRI) are the most widely used image technologies providing information associated to spinal disorders such as fractures, osteoporosis, stenosis, and masses. In recent years, there has been an increasing interest in analyzing medical images by computational methods due to the vast amount of data obtained. Therefore, these computer tools play a very important role assisting physicians not only in the diagnosis of diseases, but also in the treatment and monitoring.

Automated spine detection in CT images is an important component in many applications. For instance, the exact knowledge about spinal canal localization is essential in radiotherapy to avoid unnecessary damages of the spinal cord, which is housed and protected by spinal canal. This localization serves as initialization for automated spinal canal segmentation. Manual delineation of spinal canal is a time consuming and tedious work, so studies trying to automate this task can be found in the literature [1], [2]. Another application where spine detection is fundamental is in spine segmentation [3], [4], and hence in biomechanical modeling [5] as well as computer-aided detection (CAD) [6]. Furthermore, precise spine detection allows performing curved planar reformation and enabling easier navigation and

manipulation of spine in 3D [7]. In any case, fully automated detection in CT spine is a valuable but difficult process meantime. In addition to the common artifacts in CT images, mainly partial volume effect and noise, the most difficult challenge is to find an algorithm that can be used in patients with different abnormalities as well as in images coming from different acquisition systems with different resolution and field of view.

A considerable amount of literature has been published on this context. Štern *et al.* [8] proposed a method for automated detection of spinal centerline in CT and MR images of thoracic and lumbar spine. Their approach was based on anatomical property that the vertebral body walls have a cylindrical shape. Although they were able to localize the centerline regardless of image modality, outcome was relatively low in the upper thoracic region. In another posterior study [9], the same researchers presented a method for automated detection not only of spinal centerline, but also of vertebral bodies and intervertebral discs. Authors reported promising results; however, the method was only tested on lumbar spine. Rangayyan *et al.* [10] proposed methods to perform automatic identification of the rib structure, the spine and the spinal canal in CT images of pediatric patients. In this case, spinal canal detection was performed from the spine and ribs previously segmented. Therefore, if the segmentation is not precise, it can negatively affect the detection.

According to Major *et al.* [11], spine detection methods can be divided into two categories: **data-driven** and **anatomical model-driven** methods. The first approach uses minimal or no anatomical knowledge without machine learning whereas the latter learns characteristics of a training dataset as well as integrating a considerable amount of anatomical knowledge. Previous methods fall into the first category whereas Major *et al.* approach falls into the second one. They presented an algorithm for landmarking and labeling of spine in CT scans. Authors used 16 volumes for training and 36 for testing. The latter volumes allowed evaluating the method on three aspects: precision of the disk landmarks, correctness of the assigned labels and time performance. Following this kind of methods, Gloker *et al.* [12] presented a work for automatic localization and identification of vertebrae using regression forests and probabilistic graphical models. They used a total of 200 CT scans with different field of view. With the aim of vertebrae localization in pathological spine, a new approach was proposed by Gloker *et al.* [13]. This new method used classification forest but avoiding explicit parametric modeling of appearance. Unlike these approaches, Graf *et al.* [14] proposed a fully automatic algorithm for detecting the vertebrae without taking into account volumetric information.

The authors thank the financial support of the Spanish Ministerio de Economía y Competitividad (MINECO) and FEDER funds under Grant TEC2012-33778.

Antonio Díaz-Parra and David Moratal are at the Center for Biomaterials and Tissue Engineering, Universitat Politècnica de València, Valencia, Spain (e-mail: dmoratal@eln.upv.es).

Estanislao Arana is at the Radiology Department, Fundación Instituto Valenciano de Oncología, Valencia, Spain.

Moreover, they labeled the detected vertebrae to determine the body region under study.

Anatomical model-driven methods have the advantage of being able to detect the whole spine (including the sacrum) with a high accuracy. However, they require a training dataset and hence a great amount of *prior* knowledge, which is not always available.

In this paper, we propose a fully automated data-driven method for spinal canal detection in CT images, combining 2D and 3D information. Compared to the data-driven method just cited, our method is able to deal with both thoracic and lumbar level and no segmented reference, as spine or ribs, is needed. The only prior-knowledge that our approach uses is that spinal canal is surrounded by cortical bone in each axial cross-section.

II. MATERIAL AND METHODS

A. Material

The method was tested on two different groups of patients. The main properties of data set are presented in Table I. Group 1 consisted of 15 oncological patients (age ranging from 30 to 80) acquired on a Siemens Sensation 40 scanner at *Fundación Instituto Valenciano de Oncología (IVO)*, Valencia, Spain. On the other hand, group 2 consisted of 10 trauma patients (age ranging from 16 to 35) acquired on a Siemens Sensation 64 scanner at the Department of Radiological Sciences, University of California, Irvine, School of Medicine, USA, from Yao *et al.* [15]. The latter studies can be downloaded from a collaborative platform for research on spine imaging [16]. Thus, a total of 25 patients and 8704 images spanning thoracic and lumbar levels were analyzed. In both groups, the size of images is 512×512 pixels.

TABLE I. PROPERTIES OF THE EVALUATED IMAGES

	Total number of images	Mean number of images per patient	In-plane resolution (min-max)	Slice thickness
Group 1	4244	283	0.72-0.93 mm	2 mm
Group 2	4460	446	0.31-0.45 mm	1 mm

The algorithm was implemented in MATLAB 2013a and ran on a HP personal computer, with Intel Core i5 processor, 2.4 GHz, 4 GB of RAM, and Windows 7 Home Premium operating system.

B. Proposed Method

The algorithm can be divided into three main steps: 1) thresholding and morphological operations, 2) 3D connectivity analysis, and 3) centroid extraction for each slice. Essentially, our approach is based on the fact that spinal canal is surrounded by cortical bone in an axial cross-section. The underlying idea is to obtain only 3D connected components (CC) or objects forming part of spinal canal. For this purpose, we took into account both 2D and 3D information. The input is a set of CT images selected by the

user and it automatically provides a point with coordinates (x, y, z) for each selected slice.

1) Thresholding and Morphological Operations

In this step, we aimed to obtain a set of 3D objects belonging to spinal canal. It is very important to emphasize that our goal is not to segment spinal canal, but to extract points that can lead to algorithm for automated spinal canal detection. Firstly, to set a high contrast between spinal canal and cortical bone surrounding it, a thresholding was applied. In a heuristic way, CT volume was thresholded at 160 HU, as seen in Fig. 1a. Next, CC analysis was performed to extract the largest object in 3D. Then, CT volume was dilated using a structuring element (SE) of cylindrical shape ($r = 3\text{mm}$, $h = 10\text{mm}$) so that in the majority of slices, spinal canal was presented as a hole, reinforcing the idea that it is surrounded by cortical bone (Fig. 1b). It could also occur that spinal canal remains opened or completely closed. Thus, information about spinal canal localization is unknown in those slices and hence it is necessary to estimate the localization by interpolation and extrapolation (step 3).

After dilatation, a logical operation *NOT* was performed in the CT volume, obtaining Fig. 1c. For each axial cross-section, the objects in contact with the border of the image were removed. The outcome of this operation is shown in Fig. 1d (this object removal was carried out in 2D, not in 3D). With the purpose of taking out sharp shapes, CT volume was closed using a cylindrical SE ($r = 1\text{mm}$, $h = 5\text{mm}$). Moreover, a dilatation with the same SE was applied to recover as many missed slices as possible and provide a better estimation in step 3. It is worth noting that in this point we have 3D objects distributed throughout the volume data, some of which can belong to the spinal canal and others not (Fig. 2a). With the aim of only extracting objects forming part of spinal canal, those smaller than 500 mm^3 were removed and then a 3D connectivity analysis was performed (step 3).

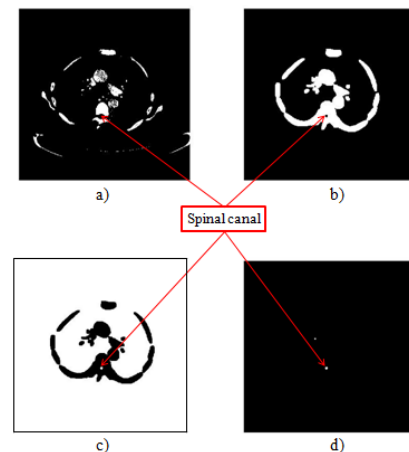


Figure 1. (a) Image thresholded at 160 HU. (b) Dilation using a cylindrical structuring element. (c) Logical operation *NOT* (image border is drawn for a better visualization). (d) Outcome of removed objects in contact with the border of the image.

2) 3D Connectivity Analysis. Linking 3D Objects

The goal of this step was to extract only those 3D objects constituting spinal canal. Each 3D object was represented by its upper and lower centroid. Setting any object as reference, the algorithm carried out a search of objects placed above and below the reference object as follows:

a) Linking upper objects to the reference object

To connect the upper objects to the reference object, a box of $20 \times 20 \times 30$ mm (length \times width \times height) was applied regarding to the upper centroid of the reference object, as seen in Fig. 2b. Thus, if the lower centroid of any object fell into the box, it was considered to be part of the same structure and hence it was linked to reference object. The search continued by defining the last linked object as the new reference. If more than one lower centroid satisfied this condition, the object with a shortest Euclidean distance between its lower centroid and the upper centroid of the previous reference object was set as a new reference. The search of upper objects ended when no lower centroid was found inside the box.

Similarly, the lower objects were linked to the reference object.

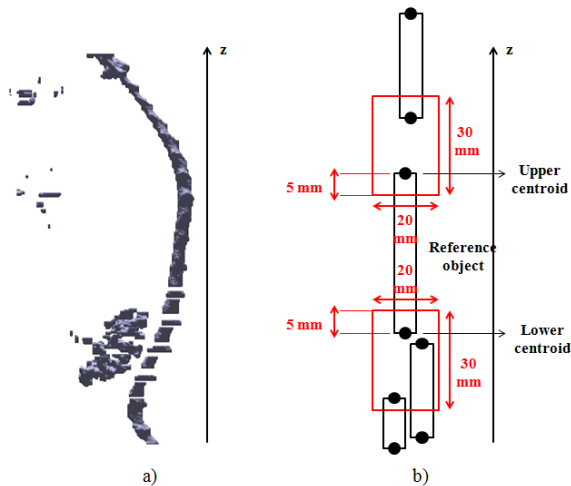


Figure 2. (a) After closing, objects can be found in 3D. Only those ones corresponding to the spinal canal are interesting for our purpose. (b) Linking process to extract only the objects constituting the spinal canal. Each object is represented by its upper and lower centroid.

b) Setting a new reference

Once the linking process has finished, i.e. the search of the objects above and below the reference object, a new object was set as a reference and a new search was carried out. Finally, when all objects were served as a reference, the evaluation of which structure corresponded to the spinal canal was performed. To determine it, we extracted the longest 3D connected object along the z axis, called the **spinal canal object**.

3) Centroid Extraction. Interpolation and Extrapolation

The last step consisted of computing the centroid of each slice constituting the *spinal canal* object. In addition, in most cases it was necessary to carry out a linear interpolation

since, as a result of the previous morphological operations, not all slices were presented in the *spinal canal* object. When this occurred at the edges of the volume data, a constant extrapolation was performed.

III. RESULTS

Fig. 3a shows the detected spinal canal in different patients from group 1. It can be observed that all points fell into the spinal canal, even when spinal canal was not completely surrounded by cortical bone. On the other hand, detection of patients from group 2 is presented in Fig. 3b. Again, all detected point lied within the spinal canal. A complete spinal canal detection of a patient from group 1 can be observed in Fig. 4.

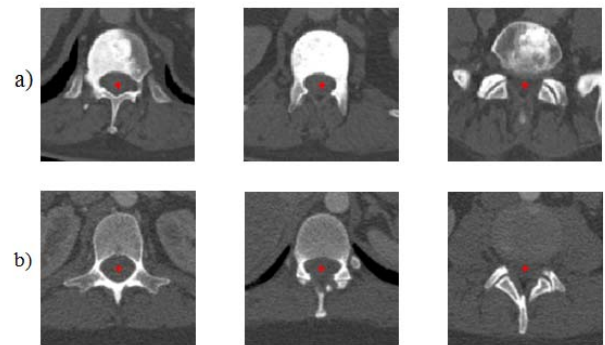


Figure 3. Outcome of spinal canal detection (red points). Detection in different patients from group 1 (a) and from group 2 (b).

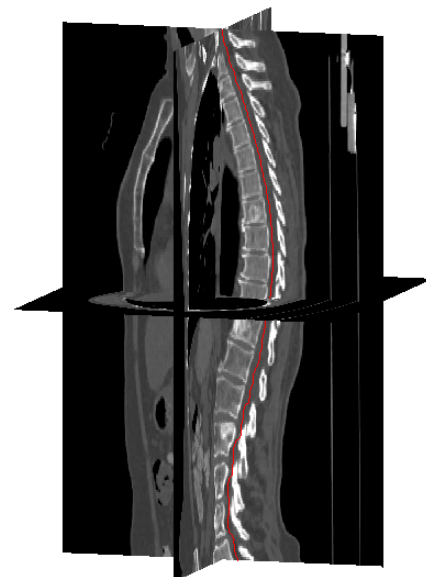


Figure 4. 3D visualization of a spinal canal detection (red line) from a patient of group 1.

The method was evaluated qualitatively by an experimented radiologist. The expert determined that all points extracted by the algorithm lied within spinal canal, what reveals the utility of the method since it lets automate the detection of the spinal canal, reducing thus the important workload that would imply a manual detection.

The computational time was 48.68 ± 14.44 s (mean \pm standard deviation) and 109.98 ± 9.80 s per patient from group 1 and 2, respectively. Therefore, the algorithm could be used for real time applications.

IV. DISCUSSION AND CONCLUSIONS

Our method is based on the anatomical property that in each axial cross-section spinal canal is surrounded by cortical bone. It was applied for detection of thoracic and lumbar levels obtaining accuracy outcome since the experienced radiologist determined that all points were localized within spinal canal. This fact suggests that our method is completely independent of the scanner used for image acquisition. Although the method was tested on thoracic and lumbar levels, some volumes selected by the radiologist included the last cervical vertebra. Therefore, we suggest that the method could detect cervical level as well.

The algorithm is able to detect spinal canal in a precise way, even when it is not completely surrounded by cortical bone, as shown in right column Fig. 3b. This is possible due to interpolation process carried out in step 3. Indeed, as a result of morphological operations (step 1) and 3D connectivity analysis (step 2), we obtain a set of points with coordinates (x, y, z) that let us estimate the localization of the spinal canal in missed slices of the *spinal canal* object.

We have focused on spinal canal detection, similar to [1]. Other studies deal with vertebral body detection rather than spinal canal, e.g. [8]. In any case, both approaches aim to detect a set of point to localize the spine, and hence automate many applications [5], [6] and make the navigation of spine in 3D easier [7].

We have proposed a method for spinal canal detection that is completely automatic. Being aware of the importance of quantitative evaluation, our future research includes it as principal task as well as comparing with other methods. For this purpose, we have several options. On the one hand, the expert could manually localize the spinal canal and hence compute the mean distance between the ground truth and the outcome provided by the method, as in [8]. Another option would be that the expert segmented the spinal canal to evaluate the algorithm in terms of true positives (TP) and false positives (FP). Thus, detected points within segmented spinal canal would be TP, and FP otherwise, similar to [11]. In any way, the obtained outcome in this work suggests promising results.

REFERENCES

[1] R. M. Rangayyan, H. J. Deglint, and G. S. Boag, "Method for the automatic detection and segmentation of the spinal canal in computed tomographic images," *J. Electron. Imaging*, vol. 15, no. 3, Jul. 2006.

[2] L. G. Nyúl, J. Kanyó, E. Máté, G. Makay, E. Balogh, M. Fidrich, and A. Kuba, "Method for automatically segmenting the spinal cord and canal from 3D CT images," in *Computer Analysis of Images and Patterns*, 2005, vol. 3691, pp. 456–463.

[3] J. Yao, S. D. O'Connor, and R. M. Summers, "Automated spinal column extraction and partitioning," in *3rd IEEE International Symposium on Biomedical Imaging: Nano to Macro*, 2006, pp. 390–393.

[4] Y. Kim and D. Kim, "A fully automatic vertebra segmentation method using 3D deformable fences," *Comput. Med. Imaging Graph.*, vol. 33, no. 5, pp. 343–52, Jul. 2009.

[5] J. Huang, F. Jian, H. Wu, and H. Li, "An improved level set method for vertebra CT image segmentation," *Biomed. Eng. Online*, vol. 12, no. 1, p. 48, May 2013.

[6] J. E. Burns, J. Yao, T. S. Wiese, H. E. Muñoz, E. C. Jones, and R. M. Summers, "Automated detection of sclerotic metastases in the thoracolumbar spine at CT," *Radiology*, vol. 268, no. 1, pp. 69–78, Jul. 2013.

[7] T. Vrtovec, B. Likar, and F. Pernuš, "Automated curved planar reformation of 3D spine images," *Phys. Med. Biol.*, vol. 50, no. 19, p. 4527, Sep. 2005.

[8] D. Štern, T. Vrtovec, F. Pernuš, and B. Likar, "Automated determination of spinal centerline in CT and MR images," in *Medical Imaging 2009: Image Processing*, 2009, vol. 7259.

[9] D. Štern, B. Likar, F. Pernuš, and T. Vrtovec, "Automated detection of spinal centrelines, vertebral bodies and intervertebral discs in CT and MR images of lumbar spine," *Phys. Med. Biol.*, vol. 55, no. 1, p. 247, Dec. 2010.

[10] S. Banik, R. M. Rangayyan, and G. S. Boag, "Automatic segmentation of the ribs, the vertebral column, and the spinal canal in pediatric computed tomographic images," *J. Digit. Imaging*, vol. 23, no. 3, pp. 301–322, Jun. 2010.

[11] D. Major, J. Hladůvka, F. Schulze, and K. Bühler, "Automated landmarking and labeling of fully and partially scanned spinal columns in CT images," *Med. Image Anal.*, vol. 17, no. 8, pp. 1151–1163, Dec. 2013.

[12] B. Glocker, J. Feulner, A. Criminisi, D. R. Haynor, and E. Konukoglu, "Automatic localization and identification of vertebrae in arbitrary field-of-view CT scans," in *Medical Image Computing and Computer Assisted Intervention*, vol. 7512, N. Ayache, H. Delingette, P. Golland, and K. Mori, Eds. Springer Berlin Heidelberg, 2012, pp. 590–598.

[13] B. Glocker, D. Zikic, E. Konukoglu, D. R. Haynor, and A. Criminisi, "Vertebrae localization in pathological spine CT via dense classification from sparse annotations," in *Medical Image Computing and Computer Assisted Intervention*, vol. 8150, K. Mori, I. Sakuma, Y. Sato, C. Barillot, and N. Navab, Eds. Springer Berlin Heidelberg, 2013, pp. 262–270.

[14] F. Graf, H.-P. Kriegel, M. Schubert, M. Strukelj, and A. Cavallaro, "Fully automatic detection of the vertebrae in 2D CT images," in *Medical Imaging 2011: Image Processing*, 2011, vol. 7962.

[15] J. Yao, J. E. Burns, H. Munoz, and R. M. Summers, "Detection of vertebral body fractures based on cortical shell unwrapping," in *Medical Image Computing and Computer Assisted Intervention*, 2012, vol. 7512, pp. 509–516.

[16] spineweb.digitalimaginggroup.ca, "Spine Web." [Online]. Available: <http://spineweb.digitalimaginggroup.ca/>. [Accessed: 14-Mar-2014].